Supporting information

Hollow structural materials derived from MOFs/Polymer loaded Co-Ru alloy for Significantly Boosting Electrochemical Overall Water Splitting

Materials. 2-Methylimidazole (99%), cobalt nitrate hexahydrate ($Co(NO_3)_2·6(H_2O)$), Zinc nitrate hexahydrate, methanol (HPLC), dopamine hydrochloride (DA) and Ruthenium chloride hydrate were purchased from Aladdin and used without further purification.

Synthesis of ZIF-67. Two solutions were prepared by dissolving 1.7 mmol (498 mg) of $Co(NO_3)_2·6H_2O$ and 17 mmol (1400 mg) of 2-methylimidazole in 50 mL of methanol, respectively. Then, at room temperature, two solutions were mixed together and standing for 12 h. The light-purple products were centrifuged for 8 min (5000 rpm), washed 3 times and dissolved at 30 mL of methanol.

Synthesis of ZIF-8. The synthesis method was the same as ZIF-67. 3 mmol (892mg) of Zinc nitrate hexahydrate was dissolved in 30ml methanol. 12mmol (985mg) of 2-methylimidazole in 5 mL of methanol. Then, at room temperature, two solutions were mixed together and standing for 12 h. The products were centrifuged for 8 min (5000 rpm), washed 3 times and dissolved at 30 mL of methanol.

Synthesis of CoRu/PDA Hollow Nanostructures (CoRu/PDA HNSs). First, removing the solution containing 60 mg ZIF-67 from the above ZIF-67 solution dispersed in 55 mL of methanol; then, 10 mL of 10mg Ruthenium chloride hydrate methanol solution and 15mL of 20 mM DA methanol solution was added. After that, the mixture was stirred at 60 °C for different time (7h, 8h, 9h and 10h). The products were collected viacentrifugation for 8 min (8000 rpm), washed 3 times by methanol, and dried at 60 °C for 12 h.

Synthesis of ZnRu/PDA Hollow Nanostructures (ZnRu/PDA HNSs). The synthesis method was the same as CoRu/PDA HNSs. Simply replaced 60mg of ZIF-67 solution with 60mg ZIF-8 and the reaction time was 9h.

Synthesis of Co/PDA Hollow Nanostructures (Co/PDA HNSs). Compared to the synthesis method of CoRu/PDA HNSs, just Ruthenium chloride hydrate methanol solution was not added and the reaction time was also 9h.

Synthesis of CoRu@N-Doped Carbon Hollow Nanostructures (CoRu@NCHNSs) catalysts.

CoRu/PDA HNSs were used as precursorsto synthesize CoRu@NCHNSs catalysts. The powder of CoRu/PDA HNSs was placed in a tube furnace and heated to 750°C for 2 h in flowing Ar with a ramp rate of 5 °C·min^{-1} to prepare CoRu@ NCHNSs.

Synthesis of Co@N-Doped Carbon Hollow Nanostructures (Co@NCHNSs) and ZnRu@N-Doped Carbon Hollow Nanostructures (ZnRu@NCHNSs) catalysts. The synthesis method was the same as CoRu@N-Doped Carbon Hollow Nanostructures (CoRu@NCHNSs) catalysts.

Characterization. Hitachi H-800 and JEM-2100F electron microscopes were used to collect transmission electron microscopy (TEM) images at 200 kV with a CCD camera. A JEOL FESEM 6700F electron microscope was used to take scanning electron microscopy (SEM) images at 3 kV. Nickel-filtered Cu Kα radiation was used to perform X-ray diffraction (XRD) analysis, and the data were collected from 5 to 80° (model Rigaku RU-200B). An ESCALAB 250 spectrometer was used to perform X-ray photoelectron spectroscopic (XPS) analysis. The metal content was obtained using inductively coupled plasma-optical emission spectrometry (ICP-OES) analyzer (ELAN 9000/DRC).

Electrochemical Measurements. A CHI660E electrochemical analyzer was used to characterize all of the performances of electrocatalytic activity. A three-electrode setup was used to evaluate electrochemical measurements with a Hg/HgO (1M KOH solution) electrode as the reference electrode and a graphite rod electrode as the counter electrode. The working electrode was a glassy carbon (GC) electrode with 3 mm in diameter. Five mg of catalyst powders was dispersed in 1 mL of solution containing 0.96 mL of methanol and 40 μL of 5.0 wt % Nafion ethanol solution to prepare the catalyst suspension, followed by ultrasonication for 20 min. The above suspension (10 μL) was dropped on the polished GC electrode and then dried at room temperature. Potentials were referenced to a reversible hydrogen electrode (RHE): $E_{RHE} = E_{Hg/HgO} + 0.098 + 0.059\times$ pH. OER and HER performance was evaluated by linear sweep voltammetry (LSV) in 1.0 M KOH at a scan rate of 10 mV·s^{-1}. Long-term chronoamperometry and cyclic voltammetry (CV) scanning were used to carry out the stability tests. Electrochemical impedance spectroscopy (EIS) measurements were performed at different potentials from 10^5 to 0.1Hz. A two-electrode cell was used to perform the activity of overall water splitting in 1.0 M KOH solution.

Calculation details

1. ECSA calculations:

The electrochemical surface area (ECSA) and ECSA-normalized current density is calculated as follows[1] :

$$ECSA = C_{dl}/C_s \quad (1)$$

$$\text{ECSA-normalized current density} = \text{current density}/ECSA \quad (2)$$

where C_s was the specific capacitance and the value of C_s was 0.04 mF cm^{-2} according to related reports.

2. TOF calculations:

The turnover frequency (TOF) can be calculated according to the following equation[2] :

$$TOF = \frac{j(\eta)A}{ZnF}$$

where j(η) is the current density (A cm^{-2}) of the LSV for different catalysts; A is the geometric testing area of electrode (cm^2); Z means the number of electrons transferred (OER: Z = 4); n is the number of surface active sites (mol); F is the Faraday constant (96485 C mol^{-1}). CV measurements were conducted from 0.1-0.2 V vs. Hg/HgO at 10 mV s^{-1} in 1 M KOH solution. The absolute components of the voltammetric charges (cathodic and anodic) tested during one CV cycle were calculated ($Q_+ + Q_-$ = integral area (I in A and V in V)/scan rate (in V s^{-1})). Assuming a one electron redox process and the maximum potential window (1.23 V), this absolute charge was multiplied by 12.3 times and divided by two ($|Qmax| = 12.3 \times (Q_+ + Q_-)/2$). The maximum number of surface active sites of the catalysts could be calculated as: $n_{max} = |Q_{max}|/F$, then the minimum TOF values were obtained.

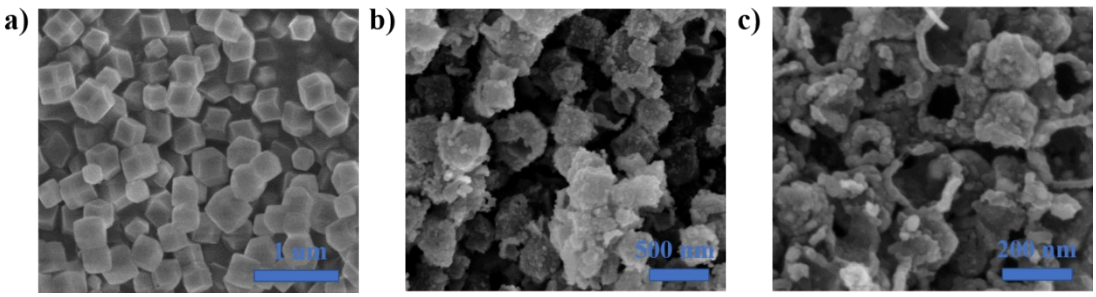

Figure S1. SEM images of the (a) ZIF-67, (b) CoRu/PDA HNSs-9h and (c) CoRu@NCHNSs-9h.

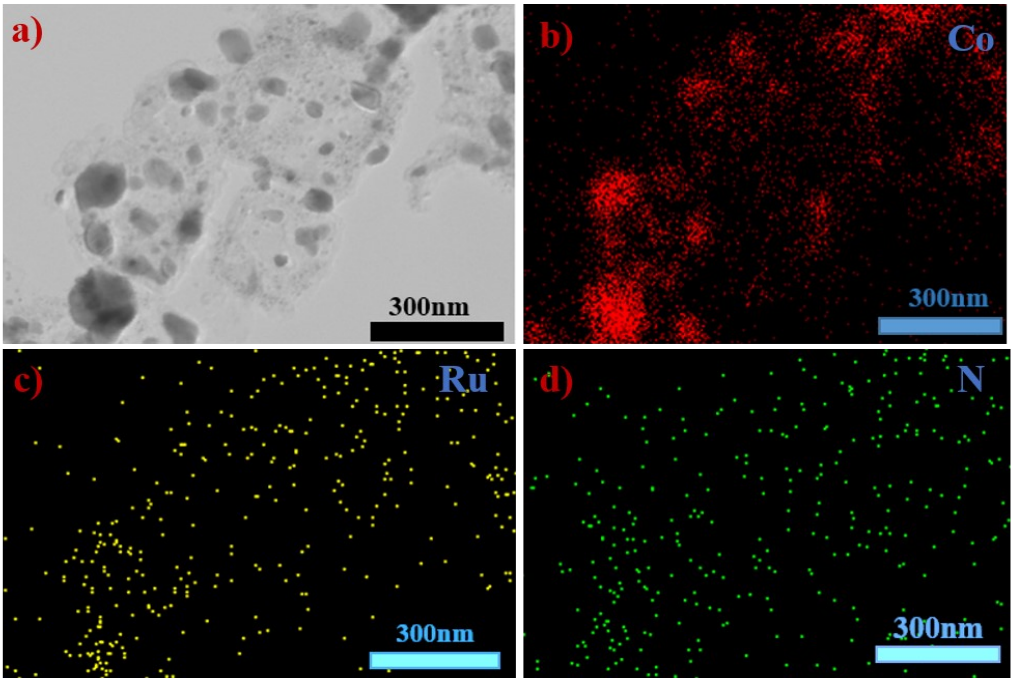

Figure S2. (a) TEM images of CoRu@NCHNSs-9h, (b-d) corresponding mapping images of CoRu@NCHNSs-9h.

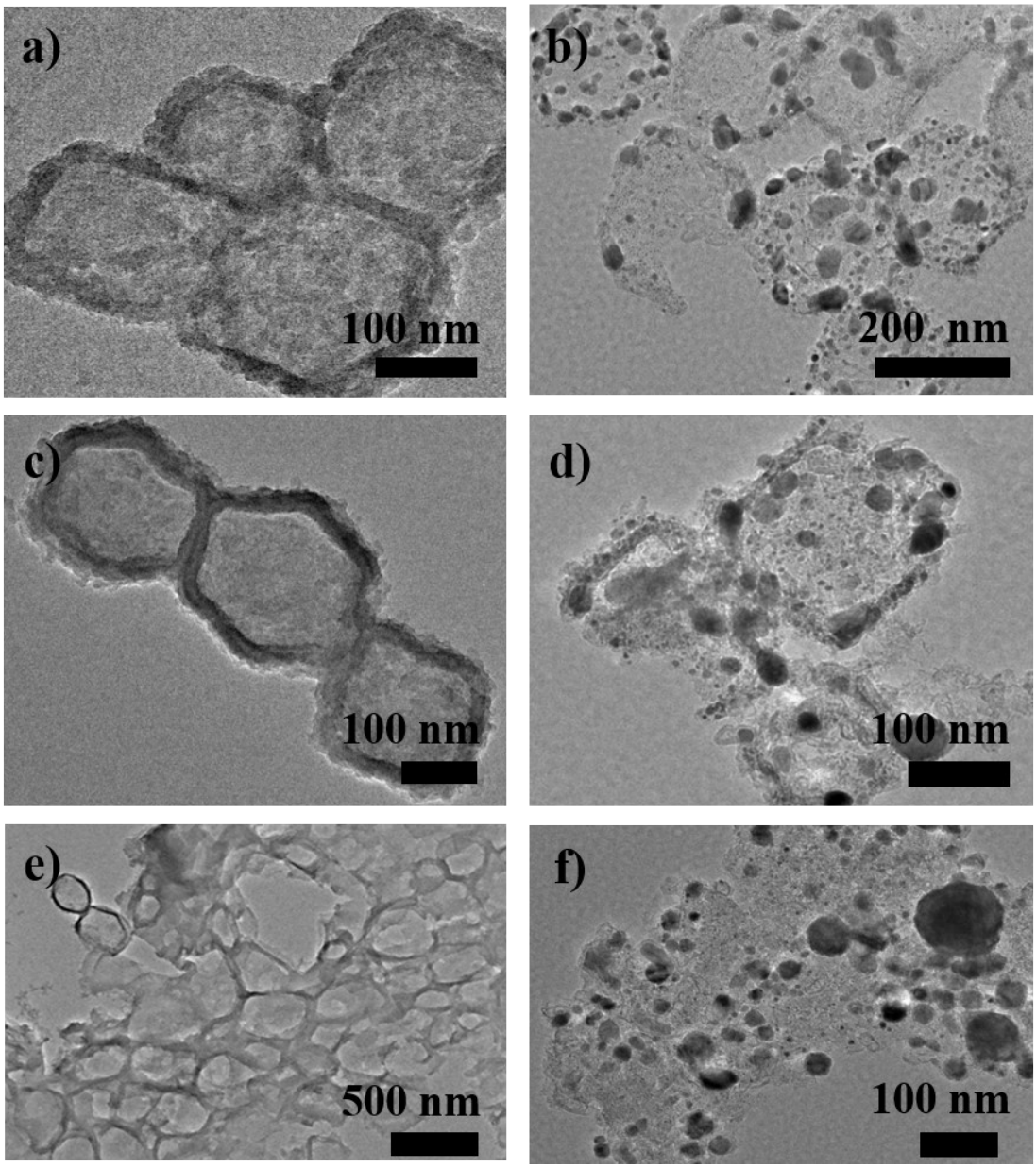

Figure S3. TEM images of (a) the CoRu/PDA HNSs-7h, (b) CoRu@NCHNSs-7h, (c) CoRu/PDA HNSs-8h, (d) CoRu@NCHNSs-8h, (e) CoRu/PDA HNSs-10h, (f) CoRu@NCHNSs-10h.

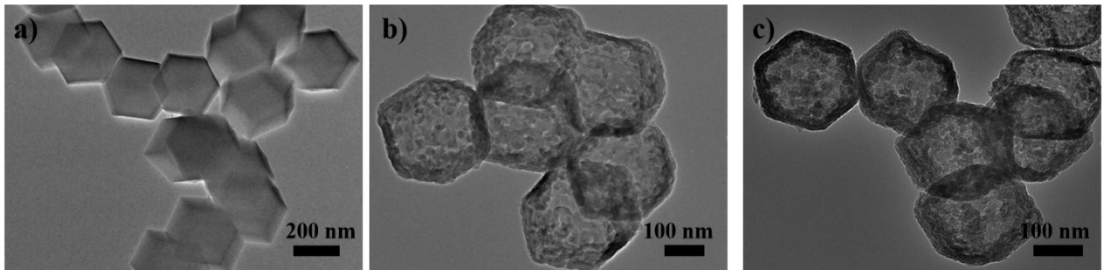

Figure S4. TEM images of the (a) ZIF-8, (b) ZnRu/PDA HNSs-9h and (c) ZnRu@NCHNSs-9h.

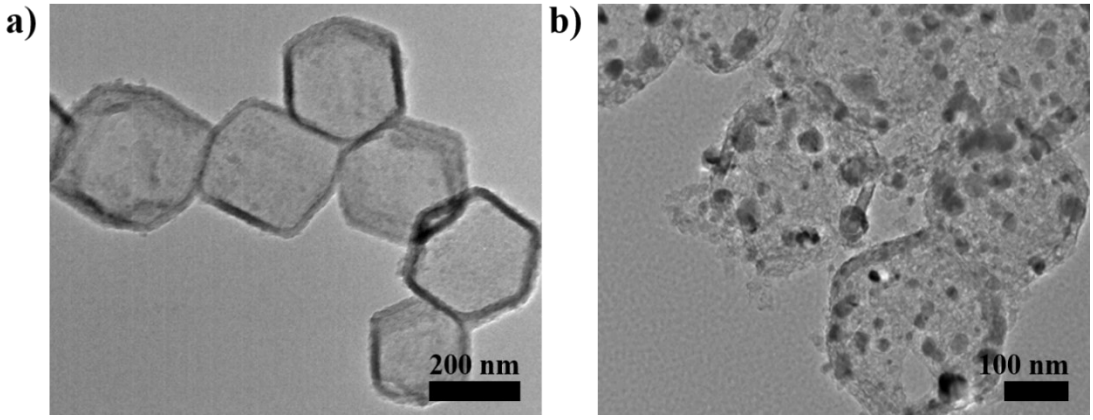

Figure S5. TEM images of the (a) Co/PDA HNSs-9h and (b) Co@NCHNSs-9h.

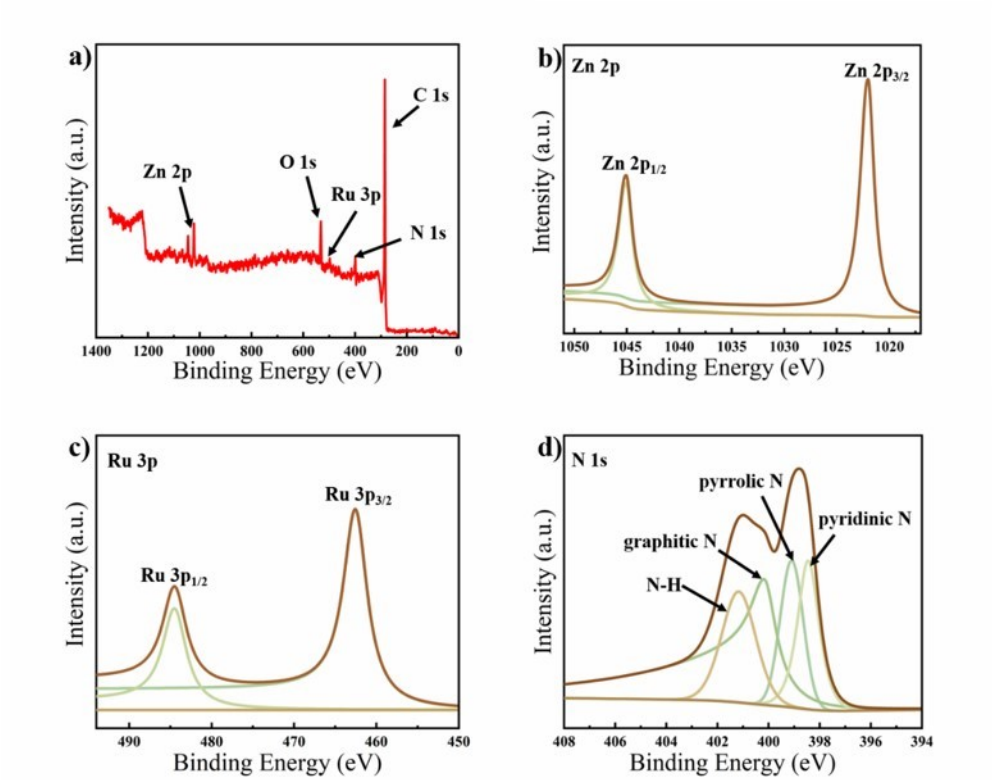

Figure S6. (a) Survey scan of the ZnRu@NCHNSs-9h, (b-d) High-resolution XPS spectra of Zn 2p, Ru 3p, N 1s.

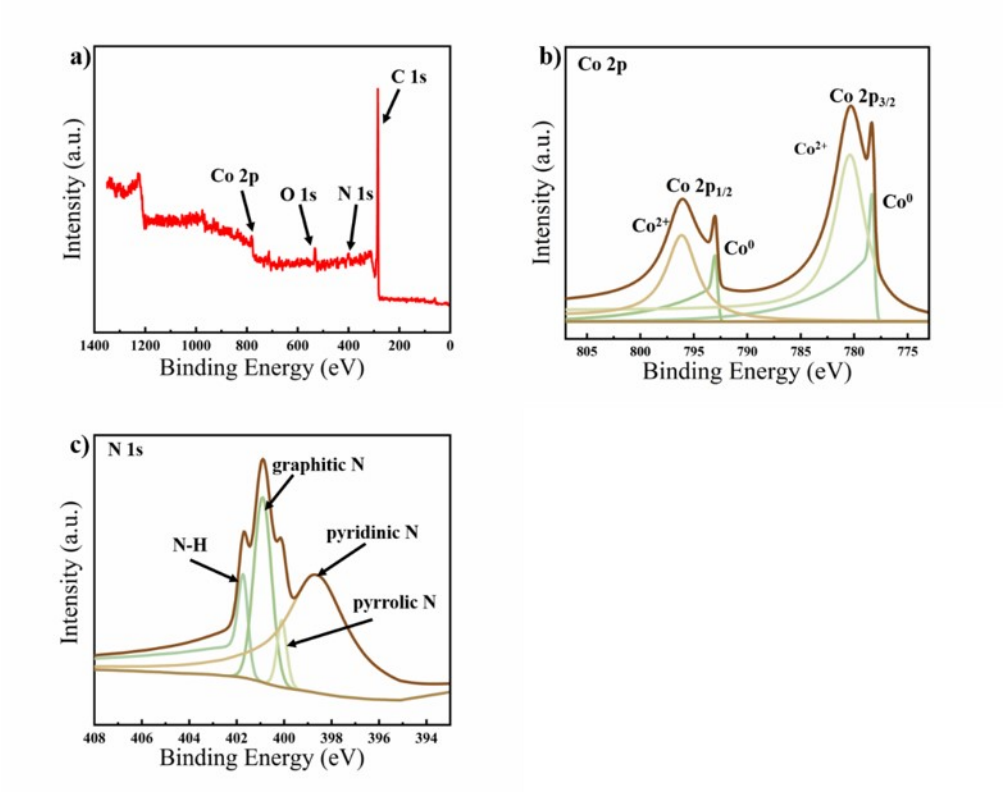

Figure S7. (a) Survey scan of the Co@NCHNSs-9h, (b-c) High-resolution XPS spectra of Co 2p, N 1s.

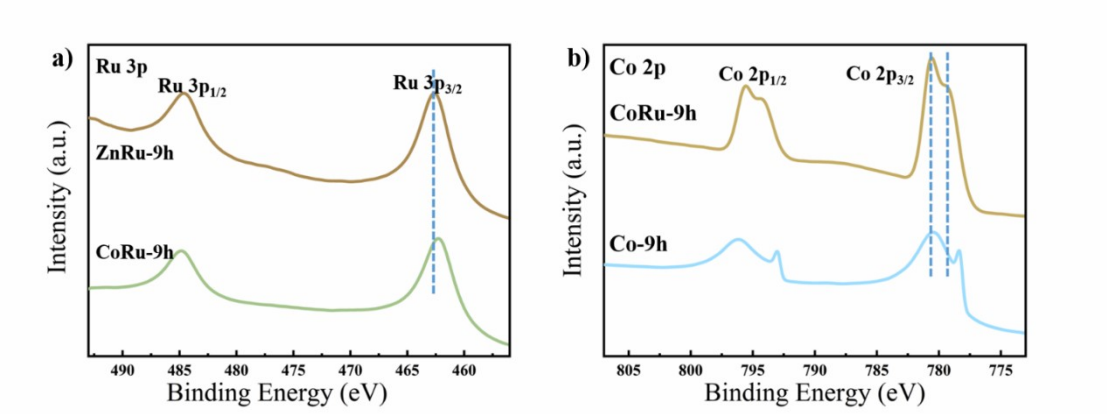

Figure S8. (a) Ru 3p high-resolution XPS spectra for CoRu@NCHNSs-9h and ZnRu@NCHNSs-9h, (b) Co 2p high-resolution XPS spectra for CoRu@NCHNSs-9h and Co@NCHNSs-9h.

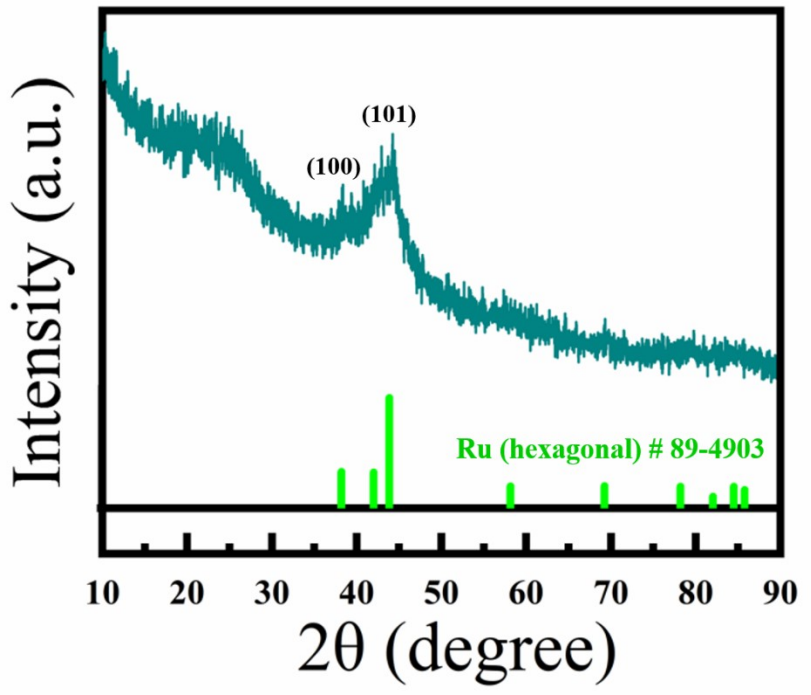

Figure S9. XRD pattern of the ZnRu@NCHNSs-9h.

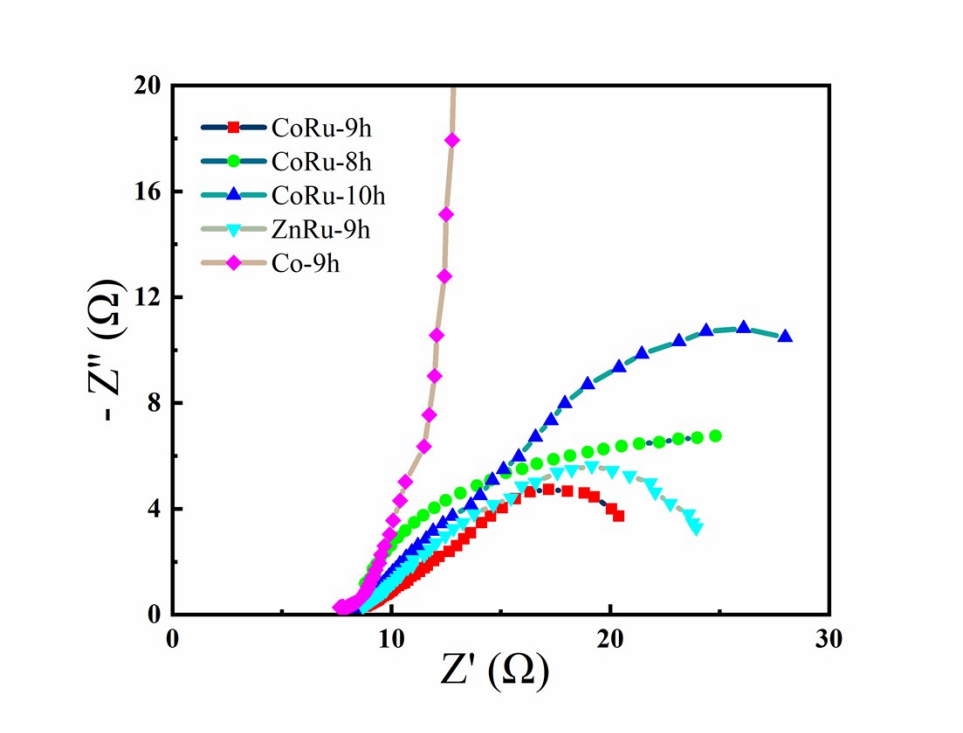

Figure S10. EIS Nyquist plots of CoRu@NCHNSs-8h, CoRu@NCHNSs-9h, CoRu@NCHNSs-10h, ZnRu@NCHNSs-9h and Co@NCHNSs-9h catalysts during HER process in 1.0 M KOH solution.

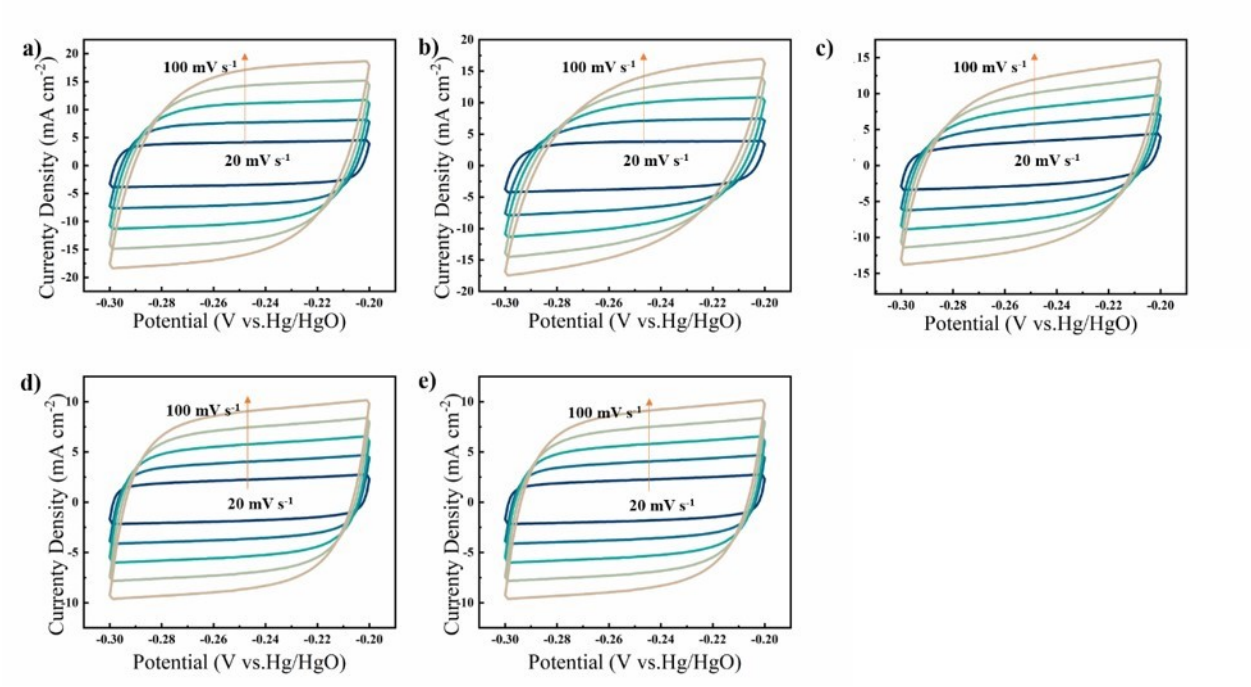

Figure S11. The CV curves at different scan rates (20-100 $mV \cdot s^{-1}$ with the interval of 10 $mV \cdot s^{-1}$) of (a) CoRu@NCHNSs-9h, (b) ZnRu@NCHNSs-9h, (c) CoRu@NCHNSs-8h, (d) CoRu@NCHNSs-10h**, (e)** Co@NCHNSs-9h catalysts during HER process in 1.0 M KOH solution.

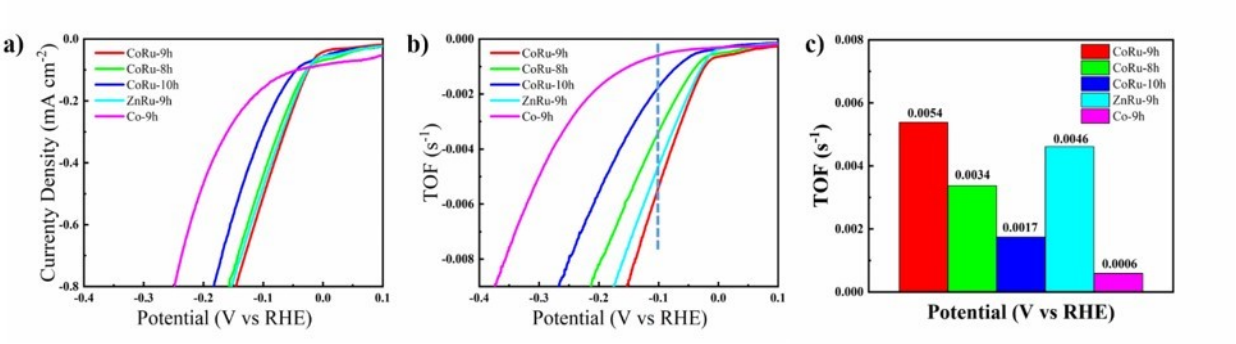

Figure S12. (a) HER specific activity curves normalized by ECSA, (b) HER TOF curves, (c) TOF value at a potential of -0.1V.

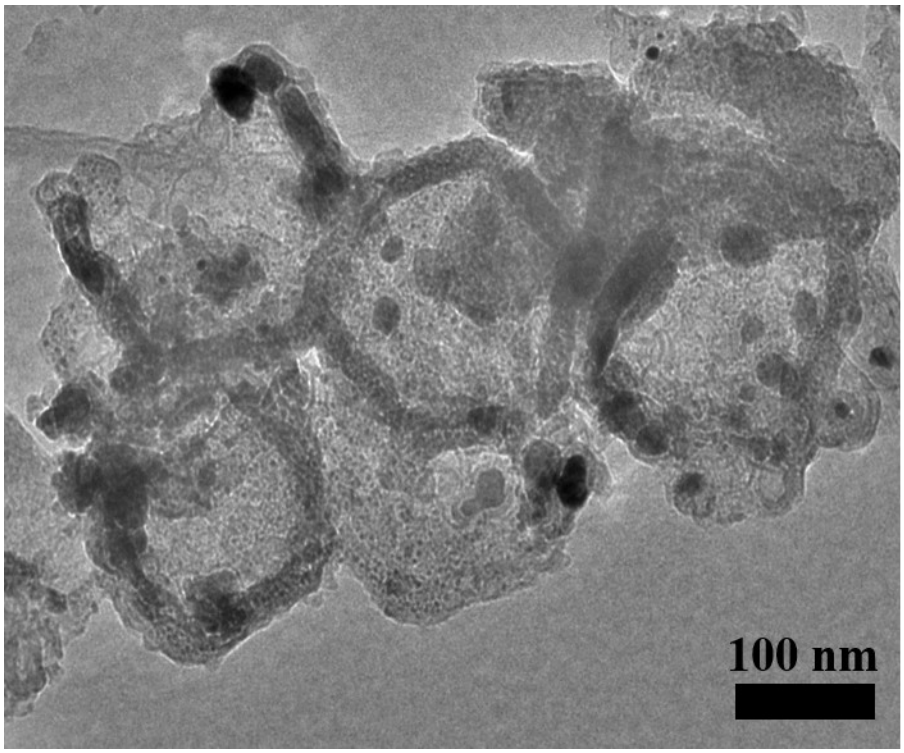

Figure S13. TEM image of the CoRu@NCHNSs-9h after HER.

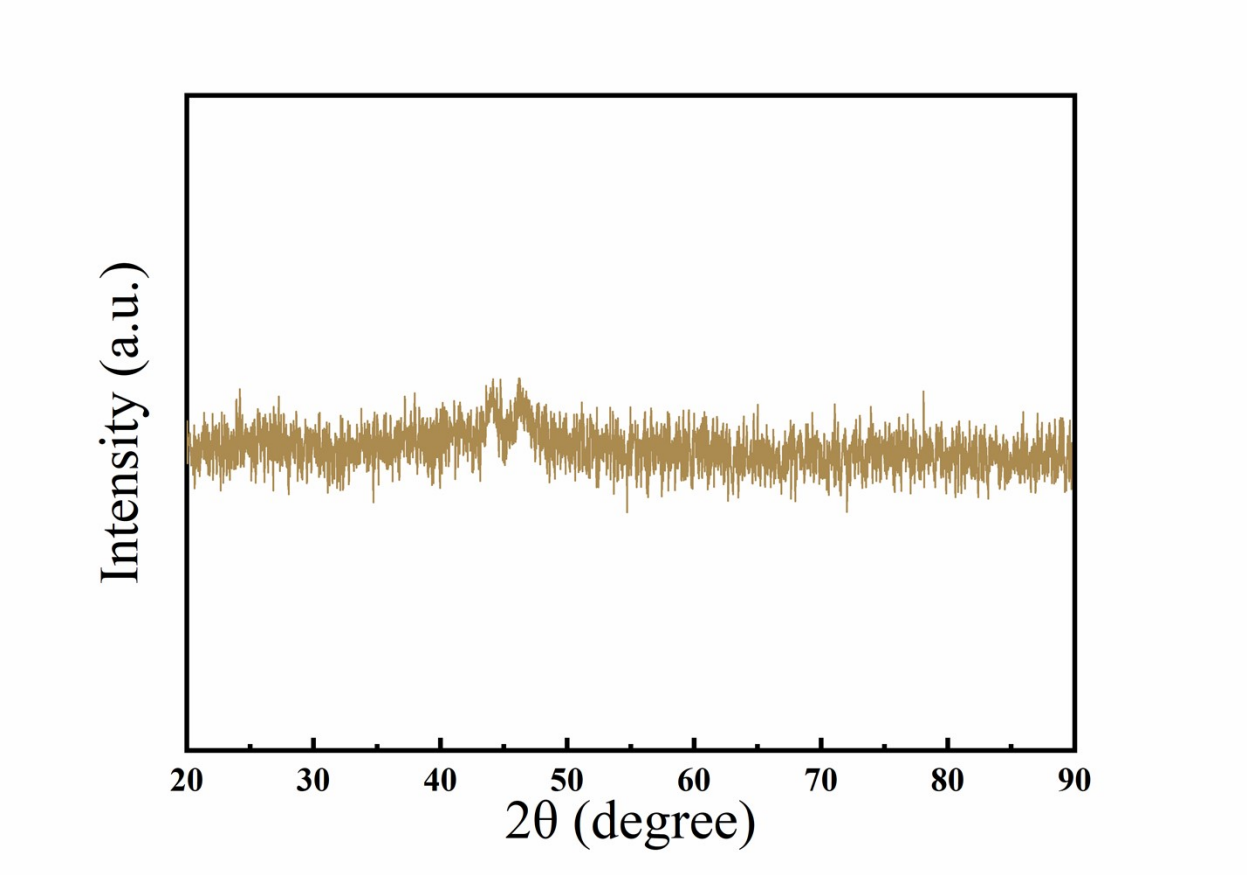

Figure S14. XRD pattern of CoRu@NCHNSs-9h after HER.

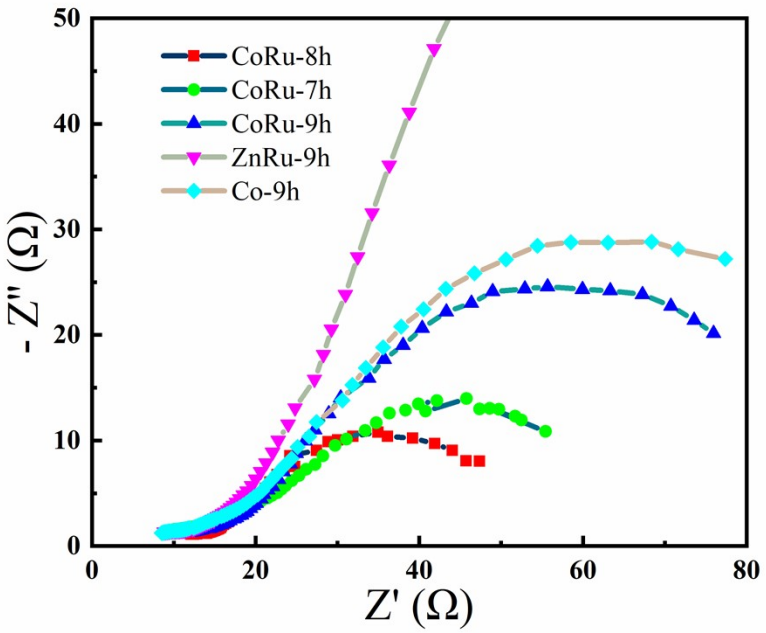

Figure S15. EIS Nyquist plots of CoRu@NCHNSs-7h, CoRu@NCHNSs-8h, CoRu@NCHNSs-9h, ZnRu@NCHNSs-9h and Co@NCHNSs-9h catalysts during OER process in 1.0 M KOH solution.

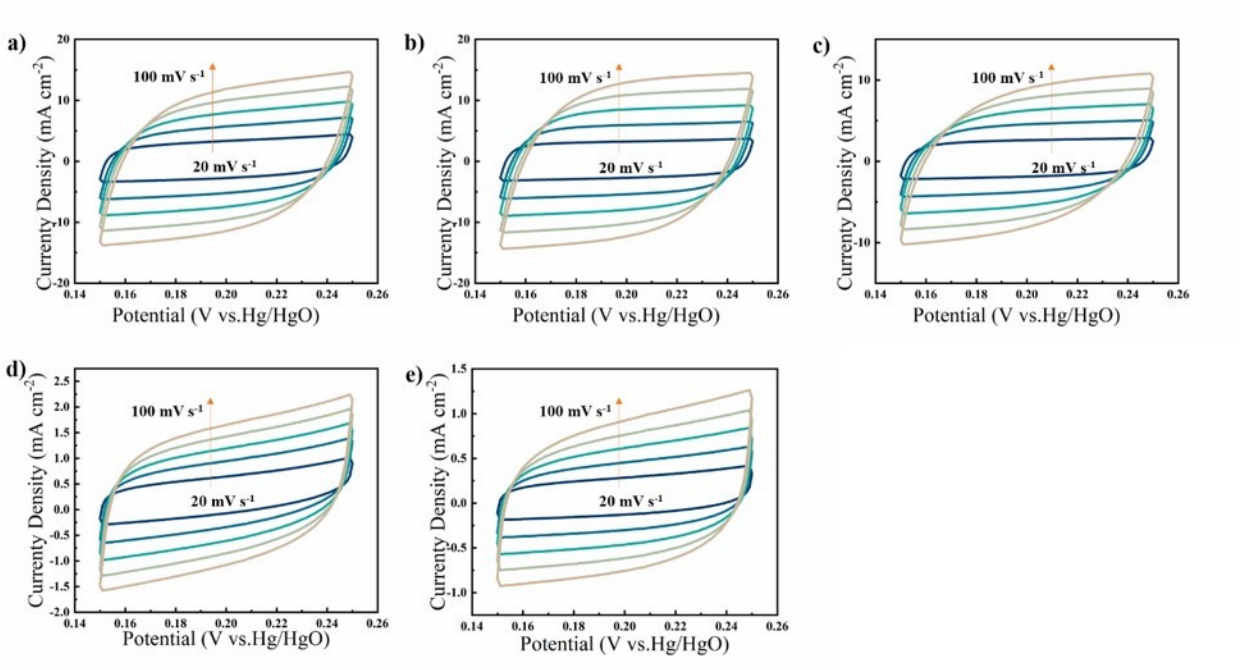

Figure S16. The CV curves at different scan rates (20-100 mV s^{-1} with the interval of 10 mV s^{-1}) of (a) CoRu@NCHNSs-8h, (b) CoRu@NCHNSs-7h, (c) CoRu@NCHNSs-9h, (d) Co@NCHNSs-9h, **(**e**)** ZnCo@NCHNSs-9h catalysts during OER process in 1.0 M KOH solution.

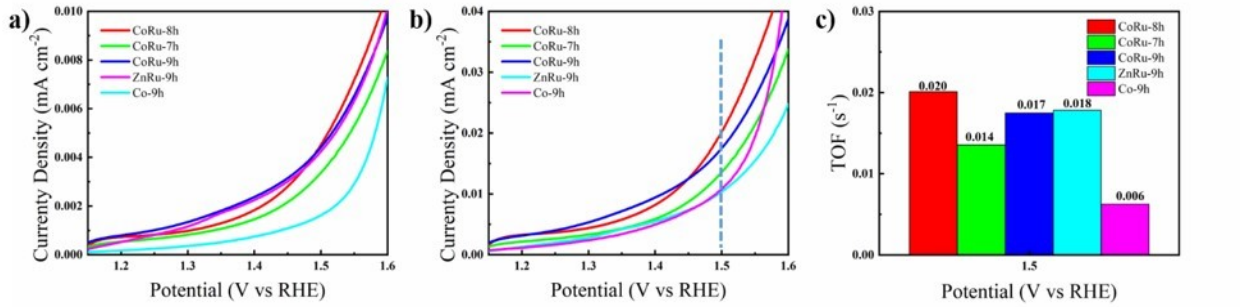

Figure S17. (a) OER specific activity curves normalized by ECSA, (b) OER TOF curves, (c) TOF value at a potential of 1.5 V.

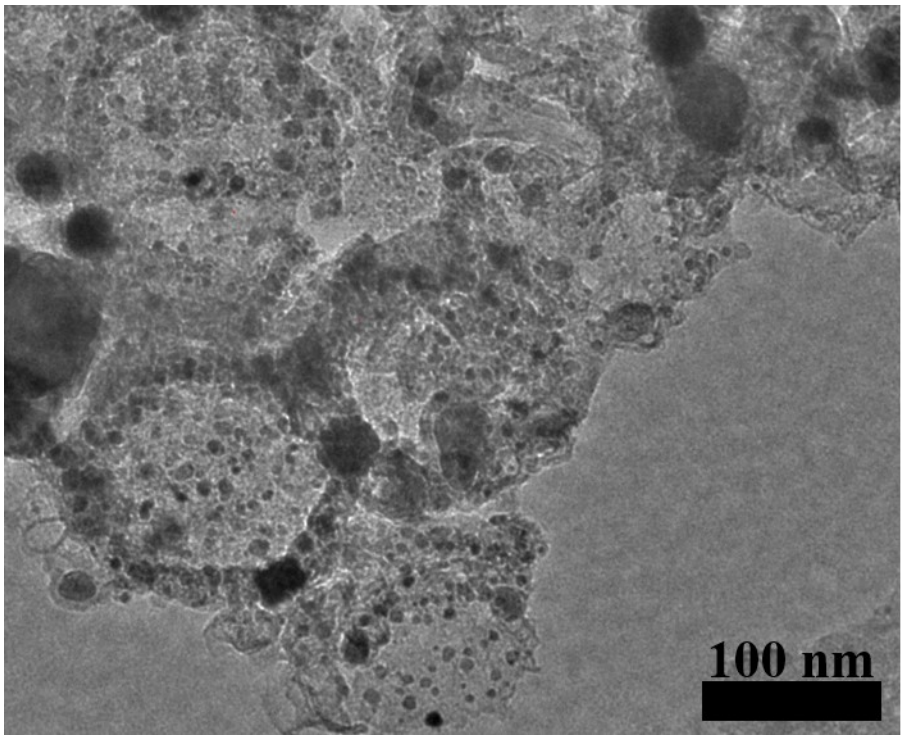

Figure S18. TEM image of the CoRu@NCHNSs-8h after OER.

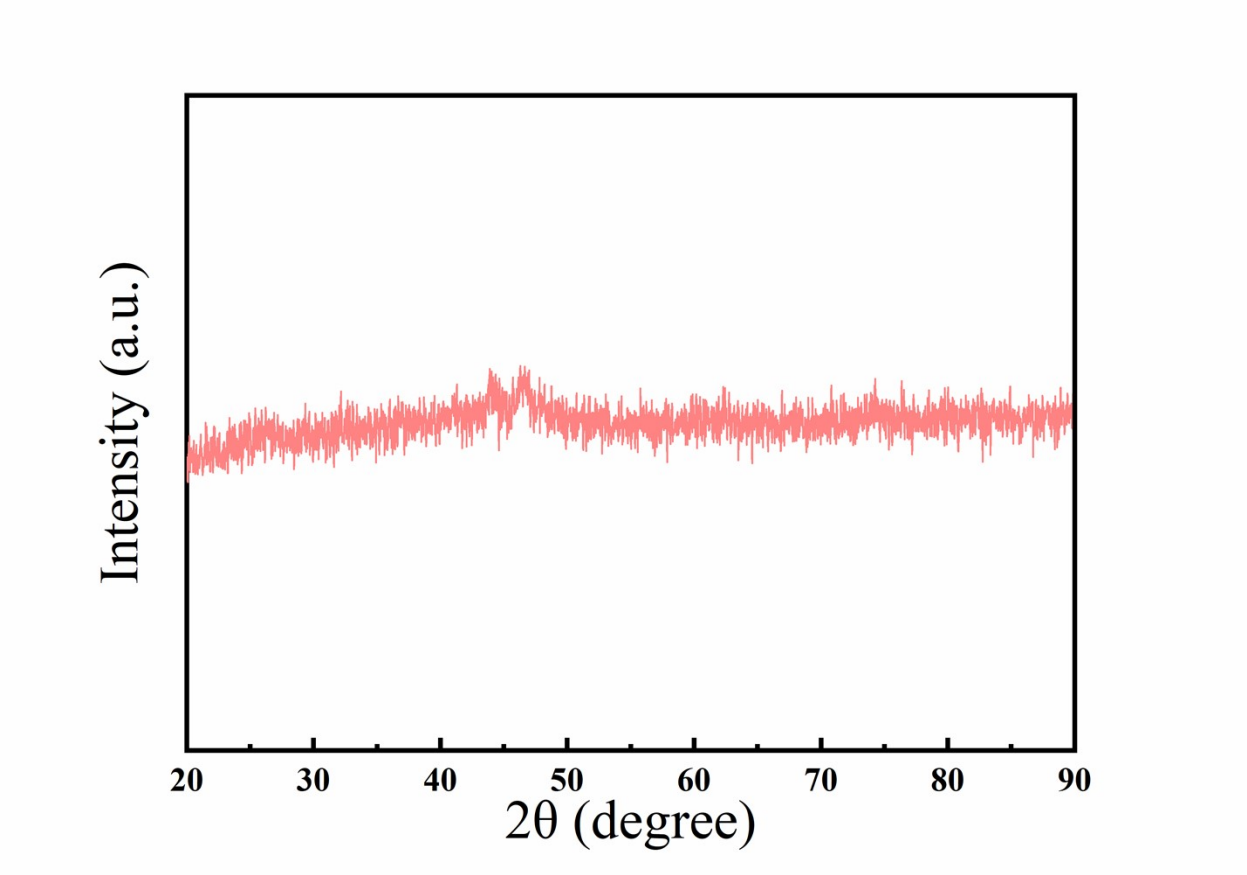

Figure S19. XRD pattern of CoRu@NCHNSs-8h after OER.

Table S1. HER performance of the CoRu@NCHNSs in this work, in comparison with other state-of-the-art non-noble metal based catalysts in 1.0 M KOH from recent publications.

Catalysts	Overpotential (mV) at 10 mA cm^{-2}	Reference
S–Fe–Ni	89	J. Mater. Chem. A, 2023, 11, 4661–4671
Pt_{SA}-NiO	55	ACS Nano 2023, 17, 18539−18547
$CoRu_{0.5}$/CQDs	18	Angew. Chem. Int. Ed. 2021, 60, 3290 – 3298
N-FeCoP	132	Small 2023, 19, 2302475
Co_7Fe_3/Co-600	68	Adv. Sci. 2023, 10, 2301961
CC/MOF-$CoSe_2$@$MoSe_2$	110	Chem. Eng. J., 2022 429 132379
NiCu/Co	68	ACS Catal. 2023, 13, 10615−10626
Co/N-$NiMo_3S_4$	78	Appl. Catal., B, 2023 338 123007
Co-OSP	132	Chem. Eng. J., 2023 465 142853
CoP/CSNSs	251	Chem. Eng. J., 2023 460 141709
Ni-Co-Fe-P NBs	32	Appl. Catal., B, 2022 310 121353
CeO_2-$NiCoP_x$/NCF	39	Appl. Catal., B, 2022 316 121678
Co-Rh_2	2	Adv. Funct. Mater. 2023, 33, 2209134
Fe_2P/Co@NPC	235	J. Mater. Chem. A, 2022, 10, 16037–16045
T-Pt-Co_4N	31	ACS Nano 2022, 16, 18038−18047
NiCoFeB	174	Adv. Energy Mater. 2023, 13, 2203002
(CoSAs-MoS_2/TiN NRs	132	Adv. Funct. Mater. 2021, 31, 2100233
Co-Fe-P	53	Chem. Eng. J., 2021 405 127002
(Fe–Co–O/Co@NC-mNS/N	112	Small 2021, 17, 2101312
V-CoP	46	Adv. Energy Mater. 2021, 11, 2101758
CoRu@NCHNSs-9h	***13***	***This work***

Table S2. OER performance of the CoRu@NCHNSs in this work, in comparison with other state-of-the-art non-noble metal based catalysts in 1.0 M KOH from recent publications.

Catalysts	Overpotential (mV) at 10 mA cm^{-2}	Reference
Co-MOF-74@CoPc	291	J. Mater. Chem. A, 2023, 11, 8141–8149
Co-ZIF/CDs/CC	226	Small, 2023, 19, 2206723
CoMM SACs	351	J. Am. Chem. Soc. 2023, 145, 8052−8063
Ir/Ni-Co_3O_4	177	Adv. Energy Mater., 2023, 2302537
FeSe/Co_2P/NF	235	J. Mater. Chem. A, 2023, 11, 8330–8341
CoFe LDH HNC	238	Small, 2023, 2302556
P-Ce SAs@CoO	261	Adv. Mater., 2023, 35, 2302462
S/N-CMF@FexCoyNi1-x-y-MOF	296	Adv. Mater., 2023, 35, 2207888
M-NiA-CoN	180	Adv. Funct. Mater., 2023, 33, 2302014
1-Co	390	Angew. Chem. Int. Ed., 2023, 62, e202305938
H-2D Co/Mo_2C@NC	256	Chem. Eng. J., 2022 435 134815
SnPi@CoP-Ni_5P_4/NCF	180	J. Mater. Chem. A, 2022, 10, 13448–13455
FeCoNiMo HEA	250	ACS Catal., 2022, 12, 10808−10817
O-Co-N/C	290	Adv. Funct. Mater., 2022, 32, 2200763
Co-POP	340	Angew. Chem. Int. Ed., 2022, 61, e202201104
$Sr_2CoIrO_{6-\delta}$	210	Adv. Funct. Mater., 2021, 31, 2104746
A-Zn/Co–Fe HNAs	226	Small, 2021, 17, 2104125
Ir-O-Co	178	Angew. Chem. Int. Ed., 2021, 60, 27126 – 27134
Fe–Co–O/Co@NC/NF	257	Small, 2021, 17, 2101312
$Sr_2Co_{1.5}Fe_{0.5}O_{6-\delta}$	318	ACS Catal., 2021, 11, 4327−4337
CoRu@NCHNSs-8h	***238***	***This work***

Table S3. ICP-OES analysis for CoRu@NCHNSs-8h and CoRu@NCHNSs-9h.

Samples	Elements	Wt%	Atomic ratio
CoRu-8h	Co	17.44	10.48
	Ru	2.85	1
CoRu-9h	Co	16.86	9.82
	Ru	2.94	1

Table S4. overall water splitting performance of the CoP NB in this work, in comparison with other state-of-the-art non-noble metal based catalysts in 1.0 M KOH from recent publications.

Catalysts	Overpotential (V) at 10 mA cm^{-2}	Reference
A-CFWO	1.55	J. Mater. Chem. A, 2021, 9, 9753–9760
Co_7Fe_3/Co	1.5	Adv. Sci., 2023, 10, 2301961
NiCu/Co	1.46	ACS Catal., 2023, 13, 10615−10626
$Co(OH)_2$/$La(OH)_3$@Cu NWs	1.56	J. Mater. Chem. A, 2023, 11, 4355–4364 |
Pt@LDH	1.49	Small, 2023, 19, 2207044
CoO/ CoP-NC	1.53	J. Mater. Chem. A, 2023, 11, 3136–3147
Co_7Fe_3/Co	1.50	Adv. Sci., 2023, 10, 2301961
$Fe_{1.2}(CoNi)_{1.8}Se_x$	1.55	Adv. Energy Mater., 2023, 13, 2300837
MOF-MoSAWSA	1.50	Nano Energy ,2023 112 108450
CoP–Ni_5P_4/NF	1.47	J. Mater. Chem. A, 2023, 11, 1801–1809
Co-NC@Ni_2Fe-LDH	1.55	Small, 2022, 18, 2107739
Sn_4P_3/Co_2P SCNAs	1.56	Appl. Catal., B, 2022 304 120923
MoS_2/$NiPS_3$	1.64	Adv. Mater., 2022, 34, 2203615
Ni_2P/WS_2/Co_9S_8@C	1.48	Chem. Eng. J., 2022 406 136961
$MoSe_2$@$NiCo_2Se_4$	1.51	Small, 2022, 18, 2200622
CuN_xCo_x/NF	1.53	J. Mater. Chem. A, 2022, 10, 15520–15527
Co-Ni_3S_2	1.54	Small, 2021, 17, 2102097
Ni_2P−CuP_2	1.45	ACS Nano, 2021, 15, 5586−5599
Fe–Ni_2P@PC/Cu_xS	1.62	Nano Energy, 2021 84 105861
NCNT-NP@NF	1.54	ACS Catal., 2021, 11, 4327−4337
CoRu@NCHNSs	***1.56***	***This work***

Reference of Supporting information

1. S. Liu, S. Geng, L. Li, Y. Zhang, G. Ren, B. Huang, Z. Hu, J.-F. Lee, Y.-H. Lai, Y.-H. Chu, Y. Xu, Q. Shao and X. Huang, *Nat. Commun.*, 2022, **13**, 1187.
2. C. Wang and L. Qi, *Angew. Chem.-Int. Edit.*, 2020, **59**, 17219-17224.